ISIJ International, Vol. 55 (2015), No. 8, pp. 1591–1598

Changes of Aromatic CH and Aliphatic CH in In-situ FT-IR Spectra of Bituminous Coals in the Thermoplastic Range

Soon-Mo SHIN, Jin-Kook PARK and Sung-Mo JUNG*

Graduate Institute of Ferrous Technology (GIFT), Pohang University of Science and Technology (POSTECH), Cheongam-ro 77, Pohang, 790-784 Korea.

(*Received on September 20, 2014; accepted on April 20, 2015*)

The change in aromatic CH (3 030–2 950 cm^{-1}) and aliphatic CH (2 920–2 850 cm^{-1}) of raw and heated coals in the thermoplastic region was investigated by Fourier transform infrared spectroscopy (FT-IR). It was confirmed that the aliphatic CH abundant in coals of high volatiles is closely related to the maximum fluidity of raw coals. The peak area ratio of aromatic CH to aliphatic CH (A_{aroCH}/A_{aliCH}) has close relationship with mean reflectance and aromaticity of raw coals. Aliphatic CH and aromatic CH decreased while A_{aroCH}/A_{aliCH} increased with increasing temperature in the thermoplastic range. However, the decomposition trend of each coal clearly showed different features. The coal of low fluidity consumed aliphatic hydrogen to release volatile even before entering thermoplastic region while the coal of high fluidity gradually consumed aliphatic hydrogen all through the thermoplastic region even though they have similar volatiles. The difference in decomposition trend of hydrocarbon resulted in different condensation pattern. In addition, according to the application of 2D correlation spectroscopy for analyzing the spectral change of each coal in thermoplastic region, the relations between R_3CH and RCH_3 (2 910 cm^{-1}, 2 958 cm^{-1}) and between R_2CH_2 and RCH_3 (2 923 cm^{-1}, 2 958 cm^{-1}) were different. It was suggested that the coal properties was correlated with the different decomposition trend and fluidity.

KEY WORDS: coal; maximum fluidity; mean reflectance (Rm); Fourier transform infrared spectroscopy (FT-IR); in-situ measurement; aromaticity; 2D correlation spectroscopy.

1. Introduction

Coke is one of the most important materials in the blast furnace as fuel and reducing agents. The lower part of the furnace is filled with coke supporting charge materials in the upper part of the furnace and the coke simultaneously allows the melted iron ores and gases to pass through the voids among cokes. Therefore, coke quality is one of the dominant factors affecting the optimal operation of blast furnace.[1] In particular, coal price has rapidly increased as of 2005 due to the keen competition of steel industries since the coal properties in coke making process determine coke quality.

In order to improve the coke quality at lower cost, it is of great importance to blend the proper coals of optimal rank and caking properties. The reflectance, fluidity and degree of coalification of coals are widely used criteria in coal blending. The coal rank is normally evaluated in terms of its reflectance or the content of volatile matter. The fluidity and total dilatation of coals are also very important caking properties for producing coke of good quality.[2–6] Generally, coal blends of proper reflectance and fluidity provide good quality of coke. For example, the reflectance of 1.2 to 1.3% and maximum fluidity of 200 to 1 000 ddpm are the ultimate target for coal blends in the conventional process.[7]

In the coking process, the chemical and physical changes of coals in the thermoplastic range are dominant factors affecting the coke strength. In the progress of carbonization, there take place main reactions such as the cracking and aromatization and condensation.[8] That is, there occur the main chemical changes such as macromolecular structural modification, structural changes in aromatic and aliphatic groups and devolatilization in the plastic range. Coal has various chemical bonds and consists of 3D cross-linked macromolecules.[9–11] In particular, Fourier transform infrared spectroscopy (FT-IR) has extensively been employed to investigate the changes in coal structure during carbonization since FT-IR provides huge amount of valuable information on the chemical composition and structure of coals.[12–14] Numerous studies previously dealt with chemical functional groups of various coals using FT-IR.[15–19] Recently, Geng *et al*.[20] proved that there is a close relationship between the aromaticity of raw coals and the ratio of peak areas of aromatic CH and aliphatic CH (A_{aroCH}/A_{aliCH}) evaluated by simple FT-IR measurement without using solid state ^{13}C NMR. Several studies already reported that the ratio of peak areas of aromatic CH and aliphatic CH in raw coals is closely related to coal properties such as reflectance and fluidity.[21–23] However, the spectral analyses of real time change have rarely been carried out although some of the previous studies dealt with coal spectra of raw coals. Most of FT-IR researches were carried out to measure the spectra

* Corresponding author: E-mail: smjung@postech.ac.kr
DOI: http://dx.doi.org/10.2355/isijinternational.ISIJINT-2014-625

at each temperature by using the different pellets of individual coal. This method had the considerable probability of experimental error such as nonhomogeneous characteristic of coal. Some FT-IR measurements of coals were attempted to analyze the decomposition trend during coal pyrolysis, but few studies about in-situ FT-IR analysis of identical coals were performed.[24,25]

The current study was focused on the spectral changes in aromatic CH and aliphatic CH of raw and heated coals by FT-IR since they are closely related to the reflectance and fluidity of coals. An in-depth understanding of the correlation between real time change of FT-IR spectra and coal properties in the thermoplastic range could result in the improvement of extensive utilization of a variety of coals for coal blending.

2. Experimental

2.1. Materials Preparation

Table 1 shows the compositions of 23 coals sampled from the constant weight feeder in Pohang Works of POSCO. Coking coals are varied in the content of volatile matter, thermoplastic properties and geographical origin (Canada, Australia, China, USA, and Russia). Coals and coal blends of about 3 g were pulverized below 1 mm. The raw coal was dried at 60°C in vacuum atmosphere for 60 min. In the case of heated coal test, 3 g of coal was put into an alumina crucible and then isothermally heated up to 500°C employing a tube furnace for 30 min in Ar atmosphere of 1 L/min.

2.2. Apparatus and Experimental Procedure

The horizontal tube furnace with a quartz tube (60 mm-OD, 55 mm-ID, and 660 mm-Length) was employed for coal carbonization experiments. A Pt-Pt/13%Rh thermocouple mounted outside the quartz tube was used for the temperature measurement. A PID controller was used to control the temperature within ±2°C. Alumina crucibles (10 mm-height, 20 mm-width, 90 mm-length) were used to heat coals in Ar gas of 1 L/min.

The FT-IR spectrometer employed in the current study (Bruker, VERTEX 80v) has several advantages for coal analyses. The analysis speed is faster than other instruments and its sensitivity has increasingly improved with lower noise level and fast scan. In addition, it is easy to use and control every function for measurements. It has an evacuation facility which can prevent the absorption of atmospheric moisture. KBr disk pellets were used for FT-IR spectra of coal samples. KBr and coal samples used for FT-IR analyses were dried at 60°C in vacuum atmosphere for 60 min. Then 10 mg of coal and 1 000 mg of KBr were

Table 1. Properties of 23 bituminous coals used in the current study.

Coals	Proximate analysis (mass%, db)				Ultimate analysis (mass%, daf)				Maximum fluidity (log ddpm)	Mean reflectance (%)
	Inherent moisture	Ash	Volatile matter	Fixed carbon	C	H	N	O		
C01	2.4	9.1	34.1	54.4	82.0	5.8	2.1	9.6	2.56	0.72
C02	1.3	8.9	21.5	68.2	87.0	5.3	1.7	5.6	1.37	1.11
C03	2.9	8.0	33.9	55.2	82.6	5.8	1.9	9.2	1.84	0.70
C04	1.5	8.2	20.2	70.2	90.7	5.3	2.0	1.7	1.30	1.23
C05	0.9	9.4	22.3	67.4	89.2	5.3	1.2	3.9	2.25	1.16
C06	1.2	7.4	32.9	58.5	86.9	5.8	1.7	4.7	4.21	0.89
C07	0.8	8.7	17.9	72.6	91.3	5.0	1.1	2.1	0.83	1.45
C08	0.8	10.2	19.4	69.6	90.3	5.3	1.5	2.6	2.34	1.27
C09	0.9	10.6	28.1	60.4	86.1	5.5	1.6	5.5	4.01	0.93
C10	1.4	6.7	33.0	59.0	86.3	5.8	1.6	5.4	4.13	0.90
C11	1.3	6.3	19.9	72.4	87.1	5.0	1.8	5.7	1.81	1.18
C12	1.0	8.6	23.7	66.7	87.6	5.4	1.8	4.7	3.11	1.11
C13	1.2	8.0	22.0	68.9	89.4	5.2	1.9	3.2	1.51	1.13
C14	1.2	7.7	38.4	52.8	83.9	6.0	1.5	5.6	4.77	0.73
C15	2.2	9.1	35.3	53.5	83.5	6.0	2.1	7.9	2.65	0.71
C16	1.2	8.9	17.5	72.4	88.8	4.9	2.3	3.8	0.30	1.42
C17	0.9	10.5	18.3	70.3	89.2	5.1	2.0	3.1	2.03	1.42
C18	0.9	10.2	24.3	64.7	88.2	5.4	2.3	3.3	2.92	1.16
C19	0.9	10.6	24.5	64.0	87.2	5.6	2.3	4.1	3.23	1.14
C20	0.9	8.0	23.8	67.4	91.0	5.1	1.0	2.4	2.86	1.20
C21	1.5	9.2	32.4	56.9	84.3	5.7	1.6	7.4	3.06	0.86
C22	0.5	9.5	17.0	73.0	91.5	5.0	0.7	2.5	0.62	1.57
C23	1.9	8.0	36.0	54.2	82.8	5.7	1.7	8.5	3.95	0.72

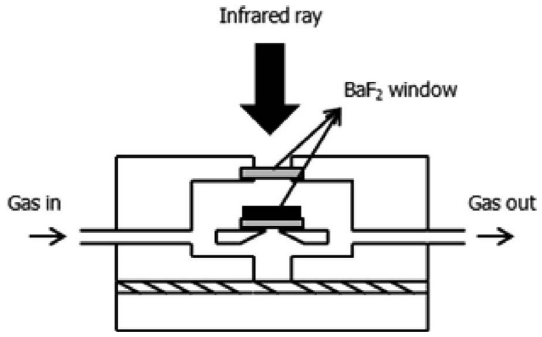

Fig. 1. Schematic diagram of the heating stage of sample for in-situ FT-IR measurement.

uniformly mixed and 8 mg of the mixture was fabricated into a disk with pressing machine (7 ton, 10 s). The disc was inserted into the sample holder and vacuum was applied in the sample box of FT-IR. The spectra were recorded by co-adding 128 scans in the wavenumber range of 4 000 to 400 cm^{-1} at a resolution of 4 cm^{-1}.

In-situ testing facility was designed as shown in **Fig. 1.** KBr disc pellet was placed in the middle of the heating stage below the BaF_2 window. ATR (Attenuated total reflection) was used to measure the change of spectra and the spectra were recorded by co-adding 64 scans in the wavenumber range for fast measurement. The pellet was pyrolyzed at the heating rate of 10°C/min in an Ar atmohsphere. The measurement interval of FT-IR was 1 min.

2.3. Two-dimensional Correlation Spectroscopy

Two-dimensional correlation spectroscopy which originated in a NMR spectroscopy has developed to analyze the results of optical spectroscopy. In 1986, Noda utilized basic theory for general 2D correlation spectroscopy. The generalized 2D correlation function is given below:

$$\Phi(\nu_1,\nu_2)+i\Psi(\nu_1,\nu_2) = \frac{1}{\pi(T_{\max}-T_{\min})}\int_0^{\infty}\tilde{Y}_1(\omega)\cdot\tilde{Y}_2(\omega)\,d\omega \quad \text{..... (1)}$$

The term $\tilde{Y}_1(\omega)$ is forward Fourier transformation of the spectral intensity variations, $\tilde{y}(\nu_1, t)$ observed at a given spectral variable, ν_1. It can be written as:

$$\tilde{Y}_1(\omega) = \int_{-\infty}^{\infty}\tilde{y}(\nu_1,t)e^{-i\omega t}dt \quad \text{..... (2)}$$

$\tilde{Y}_2(\omega)$ is defined in a similar way, but it is an inverse Fourier transform. Equation (1) will directly yield the synchronous and asynchronous correlation spectrum, $\Phi(\nu_1, \nu_2)$ and $\Psi(\nu_1, \nu_2)$.[26,27]

This method provides various advantages for the spectral analyses. First of all, it has strong deconvolution abilities. Next, it gives information about the sequence of spectral band change. The interpretation of sequence of spectral band change is fulfilled by two kinds of spectral analyses. The first part is synchronous spectrum, representing simultaneous or coincidental changes of spectral bands. The second one is asynchronous spectrum, representing sequential or successive changes of spectral bands.

2D correlation spectroscopy has been extensively used to analyze various spectra. In the current study, 2D correlation spectroscopy was applied to interpret the decomposition trend of each aliphatic CH during coal pyrolysis.

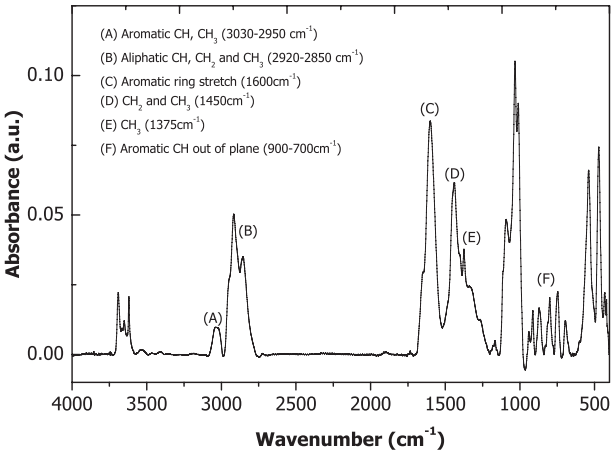

Fig. 2. FT-IR spectra of a coking coal.

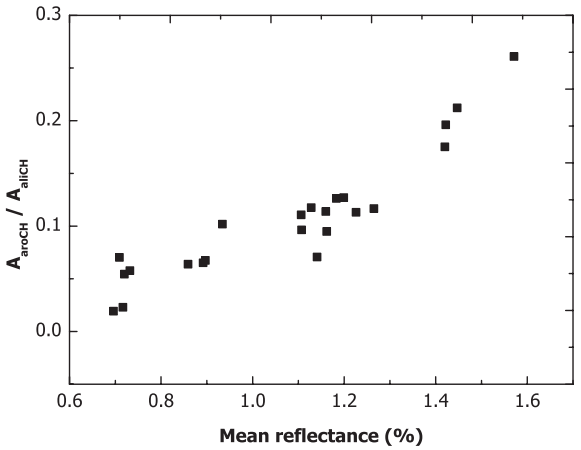

Fig. 3. Correlation between A_{aroCH}/A_{aliCH} and mean reflectance of coals.

3. Results and Discussion

3.1. Correlation between FT-IR Spectra and Coal Properties

In order to confirm the suitability of correlation between coal properties and FT-IR spectra we used, twenty-three raw coking coals were selected for the analysis. As shown in **Fig. 2**, there are several band assignments for the spectra of coals such as aromatic CH (3 030–2 950 cm^{-1}), aliphatic CH (2 920–2 850 cm^{-1}), aromatic ring stretch (1 600 cm^{-1}), CH_2 and CH_3 (1 450 cm^{-1}), CH_3 groups (1 375 cm^{-1}), aromatic CH out of plane (900–700 cm^{-1}), *etc*.[28] In the current experiments, more focus was put on aromatic CH (3 030–2 950 cm^{-1}) and aliphatic CH (2 920–2 850 cm^{-1}) and the peak areas were evaluated by integration because those functional groups are known to be closely related to the mean reflectance and coal fluidity affecting critical quality of coals.[21–23]

As shown in **Fig. 3**, A_{aroCH}/A_{aliCH} shows a close relationship with the mean reflectance which is one of the factors affecting coal rank. A_{aroCH}/A_{aliCH} increased with increasing the mean reflectance of coals, which indicates that the fraction of aromatic carbon in coal increases with increasing coal reflectance while the aliphatic hydrogen decreases.

A_{aroCH}/A_{aliCH} is also related to coal aromaticity according to the study performed by Geng *et al.*[20] They studied on the correlation between A_{aroCH}/A_{aliCH} and aromaticity of coals by FT-IR and suggested that it is possible to use A_{aroCH}/A_{aliCH} instead of the aromaticity measured by solid state ^{13}C NMR. Therefore, it was found that the aromaticity evaluated by FT-IR enhanced with increasing coal reflectance.

In a similar way, the correlation between A_{aroCH}/A_{aliCH} and atomic ratios in coals was examined because coal reflectance is closely related to the atomic ratios. As shown in **Fig. 4**, there exists a close correlation between A_{aroCH}/A_{aliCH} and the ratios of atoms in raw coals. That is, A_{aroCH}/A_{aliCH} decreased with increasing the ratios of H/C and O/C because the amount of hydrogen and oxygen decreased compared to the increased carbon in the progress of coalification. This result was also confirmed by Ibarra *et al.*[13] They derived the close relationship between the aromaticity evaluated by FT-IR and the atomic ratio of H/C. The similar results can be explained from a viewpoint of coal structure since the chemical structure of coal consists of a number of small condensed rings which are connected by the poly-methylene bridges.[10] That is, because the bridge of condensed rings normally includes hydrogen and oxygen, the atomic ratios of H/C and O/C decreased with increasing A_{aroCH}/A_{aliCH}. In conclusion, A_{aroCH}/A_{aliCH} evaluated by the FT-IR analysis can be used to estimate the coal structure such as the degree of coalification, reflectance and atomic ratio.

Coal fluidity is also one of the critical factors affecting coke quality and it is determined by the change of chemical bonding in thermoplastic range. Correlation of A_{aroCH}/A_{aliCH} with coal fluidity can also be made because coal fluidity is mainly affected by aliphatic CH and methylene groups.[21,22] As shown in **Fig. 5**, A_{aroCH}/A_{aliCH} has an approximate correlation with coal maximum fluidity quantified in terms of log ddpm and thermoplastic temperature range. That is, A_{aroCH}/A_{aliCH} approximately decreased with increasing coal fluidity and the higher A_{aroCH}/A_{aliCH} is, the narrower the thermoplastic range becomes in the current experiments. Even though the relation between Aaro/Aali and coal fluidity shows somewhat scattering tendency due to several factors affecting coal fluidity, it is believed that Aaro/Aali must be one of the important parameters determining coal fluidity as well as coal reflectance. As previously mentioned, the coals of high reflectance have a number of small condensed rings with a few bridges. This indicates that they have a close-packed structure and thus a dense structure could restrict coal fluidity due to the limited movement of chemical functional groups. From this reason, A_{aroCH}/A_{aliCH} might be related to coal fluidity to some degree. It is believed that A_{aroCH}/A_{aliCH} is weakly correlated with fluidity in comparison to the reflectance because coal fluidity is mainly affected by aliphatic CH. It is well known that the bonding energy of aromatic hydrogen (400–470 kJ/mol) is larger than that of aliphatic hydrogen (260–330 kJ/mol) and that aromatic C-H mainly starts to be broken right above the thermoplastic range.[14,29] On the other hand, most of aliphatic CH is

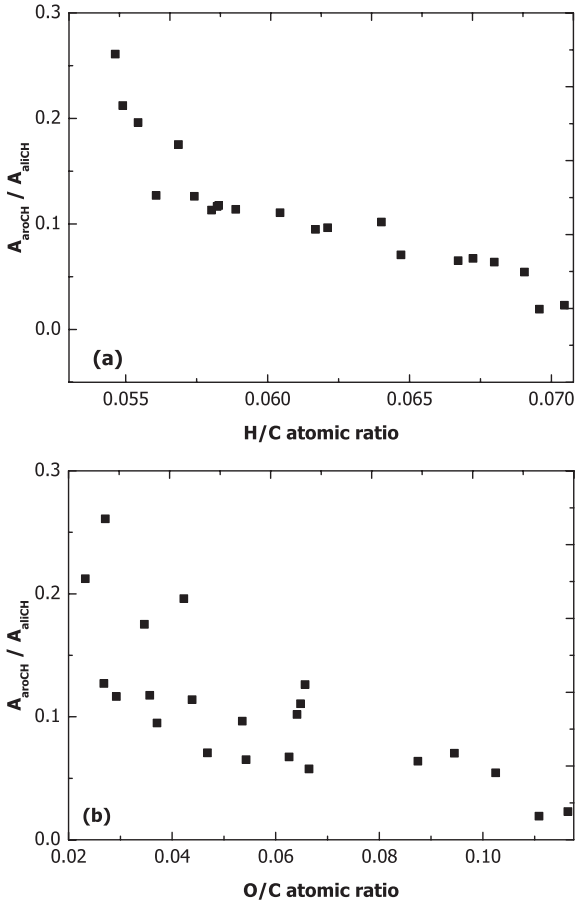

Fig. 4. Correlation between A_{aroCH}/A_{aliCH} and atomic ratio of coals. (a) A_{aroCH}/A_{aliCH} versus H/C atomic ratio. (b) A_{aroCH}/A_{aliCH} versus O/C atomic ratio.

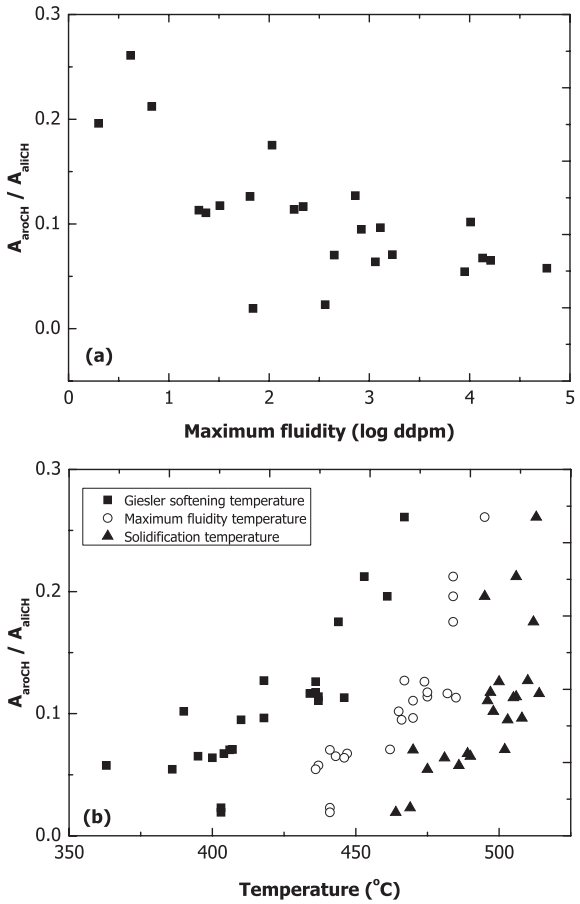

Fig. 5. Correlation between A_{aroCH}/A_{aliCH} and coal fluidity. (a) A_{aroCH}/A_{aliCH} versus log maximum fluidity. (b) A_{aroCH}/A_{aliCH} versus temperature.

mainly broken in the thermoplastic range. In conclusion, since coal fluidity is mainly affected by aliphatic CH, A_{aroCH}/A_{aliCH} is related to coal fluidity to the approximate extent.

3.2. Spectral Analyses of Heated Coals by In-situ FT-IR Measurement

3.2.1. Changes of Aromatic CH and Aliphatic CH

Figure 6 shows the decomposition patterns of CH bonds of three coals in 3 100–2 700 cm^{-1}. In the case of raw C03, it has large amount of aliphatic CH bond and small amount of aromatic CH bond, and both aliphatic CH and aromatic CH sharply dropped up to the softening temperature with increasing temperature. After the softening temperature, CH bonds steadily decomposed. On the other hand, aromatic and aliphatic CH bonds of C06 gradually diminished before the temperature entered the thermoplastic zone. It implies that the decomposition trend of C06 represents contrasting result although the amount of aromatic CH and aliphatic CH in raw coal was measured in the similar concentration to the case of raw C03. In the range between softening temperature and maximum fluidity temperature of C06, the spectral intensity rarely changed, but right above the maximum fluidity temperature, aliphatic CH started to definitely decline. However, the change of aromatic CH bond was not noticeable. In the case of C17, it showed completely different FT-IR spectra of raw coal from those of the other coals. Compared with those of C03 and C06, C17 had large amount of aromatic CH and small amount of aliphatic CH and it showed the similar decomposition behavior to C06.

Figure 7 represents the change of normalized peak areas of aromatic CH and aliphatic CH of three coals in the thermoplastic region. Normalized values were estimated with reference to the peak areas of aromatic CH and aliphatic CH in raw coals. As shown in Fig. 7(a), normalized peak area of aromatic CH for Coal C03 started to decrease at about 200°C and the value of normalized peak area decreased down to below 0.25 while those for C06 and C17 constantly decreased at smaller rates and the values converged on around 0.89 and 0.85 at the resolidification temperature, respectively. In particular, the result of C06 showed slightly unstable values due to the high fluidity and high swelling property. Swelling characteristic of coal could probably disturb the measurement of in-situ FT-IR. Therefore, it is believed that it might cause unstable results although actual aromatic CH bonds do not change. Figure 7(b) shows the change of normalized aliphatic CH. In the case of C03, aliphatic CH slightly increased above 100°C and then dropped up to 350°C drastically. In the cases of C06 and C17, they showed similar decreasing pattern above 300°C, but the aliphatic CH of C06 started to decrease earlier than that of C17. It is believed that C06 has much more weak aliphatic CH bonds than C17.

The decomposition trend of aliphatic CH to specific thermoplastic temperatures is shown in **Fig. 8**. In the case of C03, most of aliphatic CHs broke below softening temperature. This result indicates that most of transferable hydrogen acting as stabilizer of radicals were already consumed at the beginning of thermoplastic region and it caused early cross-linking to quickly form three dimensional structure before it went into the zone of high fluidity. On the other hands,

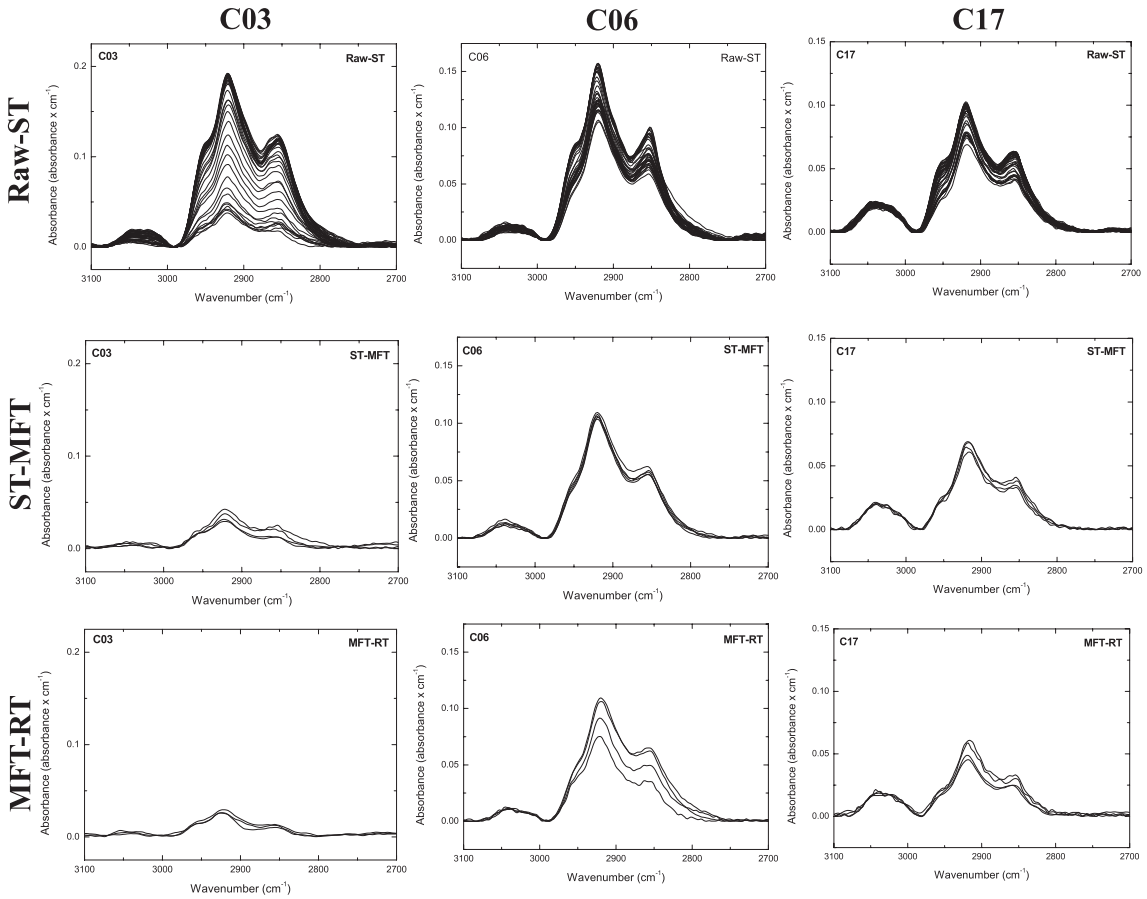

Fig. 6. Decomposition trends of three coals between 3 100–2 700 cm^{-1}.

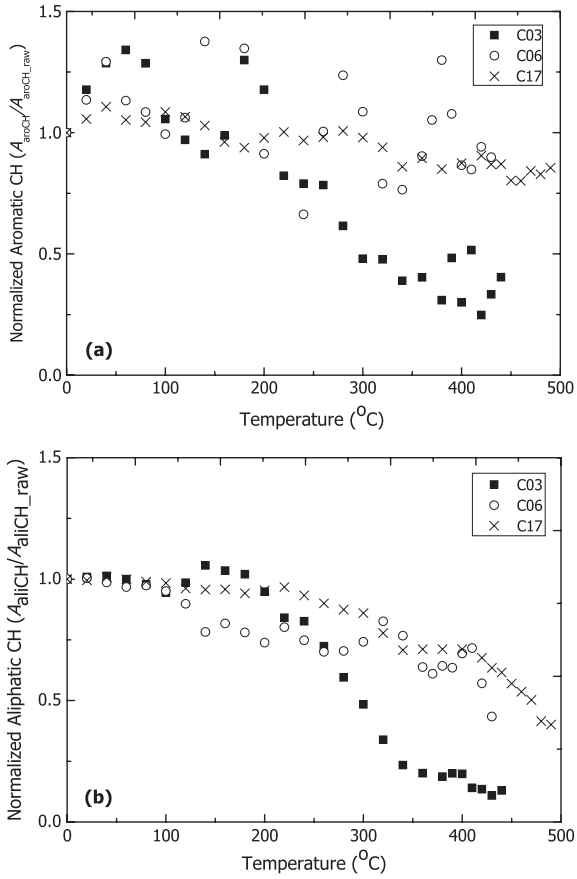

Fig. 7. Change in the normalized peak areas of aromatic CH and aliphatic CH with increasing temperature. (a) Normalized peak area of aromatic CH versus temperature. (b) Normalized peak area of aliphatic CH versus temperature.

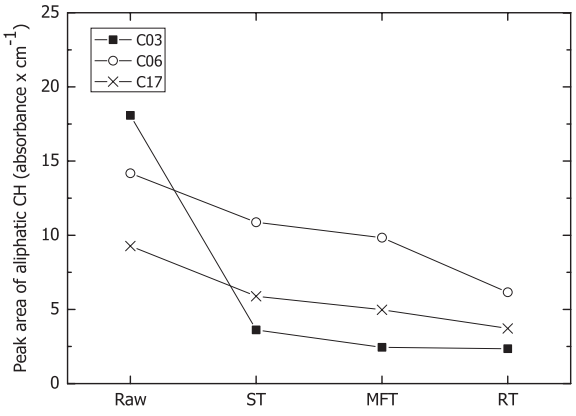

Fig. 8. Change in the amount of aliphatic CH for three coals with increasing temperature.

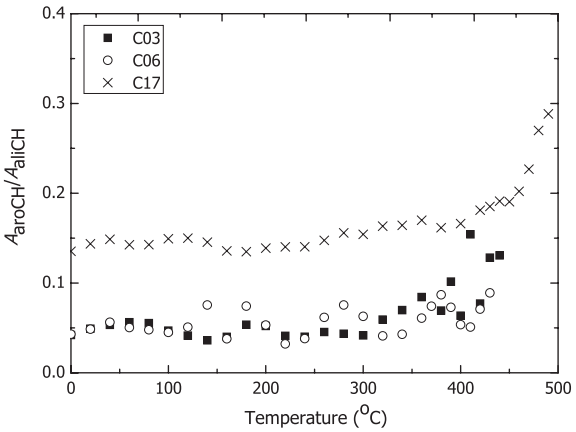

Fig. 9. Change in A_{aroCH}/A_{aliCH} with increasing temperature.

Table 2. Spectral analyses of raw coals.

Coal	VM[a]	LMF[b]	Rm[c]	SI[d]	Aromatic CH[e]	Aliphatic CHe	A_{aroCH}/A_{aliCH}[f]
C03	33.20	1.71	0.71	2.80	0.759	18.07	0.042
C06	33.04	4.21	0.88	3.47	0.609	14.17	0.043
C17	18.28	2.03	1.45	6.51	1.255	9.27	0.135

[a] Volatile matter, mass%
[b] Maximum fluidity, log ddpm
[c] Mean reflectance, %
[d] Strength Index to predict the stability factor from CBI(Composition Balance Index)
[e] Absorbance x cm^{-1}
[f] Peak area ratio for aromatic CH and aliphatic CH

C06 showed gradual or steady decomposition of aliphatic CH. Eventually, C06 had sufficient amount of aliphatic CH to stabilize the radicals at the softening temperature. It is well known by the previous research that the behavior contributes to the promotion of fluidity.[30] Although C17 had entirely opposite characteristic such as low volatile, low fluidity and high reflectance, its decomposition trend was similar to that of C06. The amount of aliphatic CH of raw C17 was lower than those of the others, but the decreasing rate was small like C06. At the softening temperature, C17 had a larger amount of aliphatic CH than C03 even though raw C17 had the smallest aliphatic CH. This result matches up with the difference of maximum fluidity of each coal. Although C03 had larger amount of aliphatic CH than C17, it had the smallest number of aliphatic CH which provided the stability of the free radicals at the beginning of thermoplastic region. Therefore, it is reasonable that insufficient amount of transferable hydrogen and early cross-linking of C03 led to the lowest fluidity, 1.71 among three coals.

3.2.2. Change of Condensation Degree during Pyrolysis

The fraction of aromatic carbon is called condensation degree, which is of great importance for determining coal rank. In this study, the condensation degrees of three coals were evaluated in terms of A_{aroCH}/A_{aliCH}. **Figure 9** indicates the change of condensation degree with increasing temperature during pyrolysis. The condensation degrees of C03 and C06 were similarly low, which was ascribed to low reflectance, 0.71 and 0.88 as shown in **Table 2**. Above 320°C, the condensation degrees of C03 and C06 started

to increase up to about 0.1 at resolidification temperature while the condensation degree of C17 started to increase at 450°C, and rapidly reached up to 0.29. It suggests that the aromatic cluster system of C17 not only develops more than those of C03 and C06 at the end of thermoplastic region, but also it has denser structure during pyrolysis. **Fig. 10** shows the change of condensation degree at specific thermoplastic temperatures. All the coals showed similar increase in the condensation degree except for the case of C03. The condensation degree of C03 decreased in the range of softening to maximum fluidity temperatures since the decomposition rate of aromatic CH was higher than that of aliphatic CH in the range. However, the condensation degree increased with rapid decomposition of aliphatic CH above the maximum fluidity temperature. The condensation degrees of C03 and C06 gradually increased and they marked the values of 0.13 and 0.089 at the resolidification temperature, respectively, representing that the polymerization of aromatic ring slowly proceeded while the condensation degree of C17 reached high value, 0.29 at the end of thermoplastic zone. It is believed that the difference might affect the structural density of formed aromatic plane during coal pyrolysis, thus it causes entirely different SI (Strength Index) as shown in Table 2.

3.3. Interpretation of Coal Pyrolysis Behavior by 2D Correlation Spectroscopy Analysis

According to the previous results, coal properties have close relationship with the decomposition trend during coal pyrolysis. It was reported that 2D correlation spectroscopy could provide more specific information about the decomposition trend of each coal in the case of its extensive application.[26,27] **Figure 11** illustrates the spectra of two coals (C03 and C06) measured by 2D correlation spectroscopy in the wavenumber range of 3 100 to 2 700 cm^{-1}. As shown in **Table 3**, the peaks at 3 050, 2 958, 2 923 and 2 910 cm^{-1} indicate aromatic CH, RCH_3, R_2CH_2 and R_3CH, respectively. All inter-correlated evaluations among the aliphatic CH peaks of C03 and C06 are arranged in **Table 4**. On the basis of Fig. 11, both coals have almost the identical synchronous spectrum pattern as represented in red color, which indicates that all the CH peaks change in the same direction. Actually, all the aliphatic CH and aromatic CH only decompose and break the bond of CH with increasing temperature. However, it was found that the asynchronous spectra of two coals such as the relationships between 2 910 and 2 958 cm^{-1} and between 2 923 and 2 958 cm^{-1} were different. In the view of 2D correlation spectroscopy, the opposite color in the identical region implies that the reaction sequence is reversed. For example, in the case of asynchronous spectra of C03, the point (2 910 cm^{-1}, 2 958

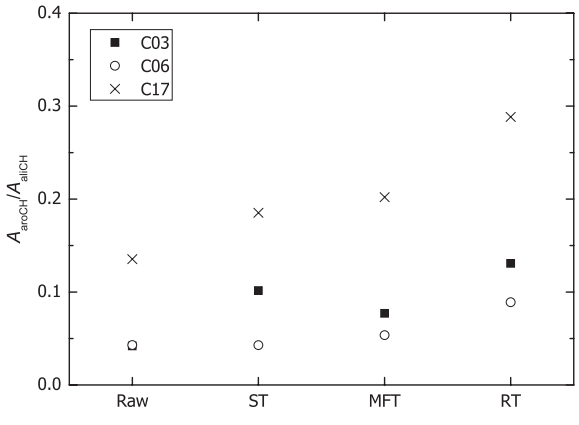

Fig. 10. Change in A_{aroCH}/A_{aliCH} for three coals.

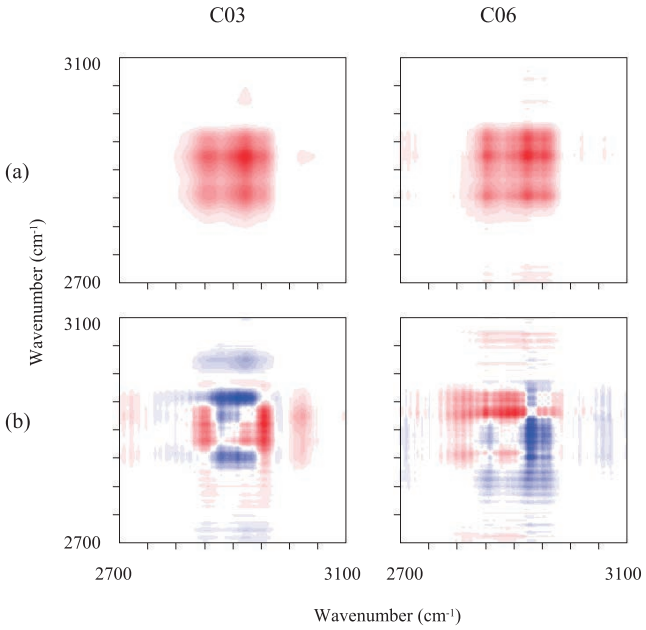

Fig. 11. (a) Synchronous spectrum and (b) asynchronous spectrum of two coals by 2D correlation spectroscopy.

Table 3. Band assignment for the infrared spectra of coals.

Centre (cm^{-1})	Width (cm^{-1})	Assignment
3 050	–	Aromatic CH
2 958	34	Asym. RCH_3
2 923	35	Asym. R_2CH_2
2 910	31	R_3CH
2 871	31	Sym. RCH_3
2 851	44	Sym. R_2CH_2

Table 4. Synchronous and asynchronous correlation of aliphatic CH for C03 and C06.

Φ(Syn)		Ψ(Asyn)		Sequence	
C03	C06	C03	C06	C03	C06
Φ (2 910,2 923) > 0	Φ (2 910,2 923) > 0	Ψ (2 910,2 923) < 0	Ψ (2 910,2 923) < 0	R_2CH_2–> R_3CH	R_2CH_2–> R_3CH
Φ (2 910,2 958) > 0	Φ (2 910,2 958) > 0	Ψ (2 910,2 958)< 0	Ψ (2 910,2 958) > 0	RCH_3–> R_3CH	R_3CH–> RCH_3
Φ (2 923,2 958) > 0	Φ (2 923,2 958) > 0	Ψ (2 923,2 958) < 0	Ψ (2 923,2958) > 0	RCH_3–> R_2CH_2	R_2CH_2–> RCH_3

Table 5. Noda's rule.[27]

Synchronous Cross-peak	Asynchronous Cross-peak	Sequence
Positive (ν_1, ν_2)	Positive (ν_1, ν_2)	ν_1 varies before ν_2
Negative (ν_1, ν_2)	Positive (ν_1, ν_2)	ν_1 varies after ν_2
Positive (ν_1, ν_2)	Negative (ν_1, ν_2)	ν_1 varies after ν_2
Negative (ν_1, ν_2)	Negative (ν_1, ν_2)	ν_1 varies before ν_2

cm^{-1}) indicates the negative value (blue color). According to Noda's rule[27] shown in **Table 5**, it suggests that R_3CH (2 910 cm^{-1}) varies after RCH_3 (2 958 cm^{-1}). However, in the case of C06, the same point (2 910 cm^{-1}, 2 958 cm^{-1}) indicates the positive value (red color) in contrast with that of C03. Thus, it indicates that R_3CH (2 910 cm^{-1}) varies before RCH_3 (2 958 cm^{-1}) in the reverse manner. According to the previous interpretation by 2D correlation spectroscopy for C03, RCH_3 starts to break before the cleavage of R_2CH_2. Two possibilities can be considered to explain the results. One of the possibilities might be the early release of methane by the breakage of weak C-C bond. The early release of methane results in the release of some C-H bonds connected to RCH_3, which shows the early decrease in the total aliphatic hydrogen. The other possibility is that the length of aliphatic hydrocarbon shows temporary increase actually because the methylene bridge might increase a little at the initial stage of decomposition as C-H bond of RCH_3 is broken and that it forms longer chains with combining with other radicals. It might result in forming numerous structures of long hydrocarbon. This is because the concentration of aliphatic CH quickly drops above about 150°C, which is the initiation of hydrocarbon collapse as numerous bridges of unstable weak methylene start to be broken as shown in Fig. 7. On the other hand, completely opposite result to that of C03 was obtained in the case of C06. First of all, the length of aliphatic hydrocarbon is shortened as the methylene bridges are broken. Then RCH_3 is broken and aliphatic CH is gradually decreased. This decomposition trend probably leads to the gradual decrease in aliphatic CH at small decreasing rates. Therefore, according to these results, aromaticity (A_{aroCH}/A_{aliCH}) of raw coal is not only important factor on coal fluidity, but the pattern of decomposition during coal pyrolysis also has significant effect on coal fluidity.

4. Conclusions

The current investigation was carried out to establish some relationships between FT-IR spectra of functional groups and coal properties. From the findings, the following conclusions were obtained:

(1) It was confirmed that A_{aroCH}/A_{aliCH} has good relationship with coal reflectance, but it is approximately related to coal fluidity because aliphatic hydrogen affects coal fluidity more than aromatic hydrogen.

(2) High volatile coals have high amount of aliphatic CH, which results in low A_{aroCH}/A_{aliCH}. This indicates that high volatile coals have high fluidity due to the abundance of aliphatic CH which is easily broken in the thermoplastic range.

(3) It was shown that numerous aliphatic CH bonds in the semi soft coking coal (C03) break prior to the thermoplastic range. It promotes early cross-liking and radical recombination, which results in low fluidity. Two kinds of hard coking coals (C06, C17) showed sufficient hydrogen at softening temperature, which could be used to stabilize radicals in the thermoplastic range.

(4) Coals increase in condensation degree with increasing temperature during pyrolysis. Hard coking coal with high reflectance and low volatiles shows higher condensation degree at the end of thermoplastic zone.

(5) According to the analyses by 2D correlation spectroscopy, during the pyrolysis of semi soft coking coal with low fluidity, RCH_3 bond started to break before the cleavage of R_2CH_2 and R_3CH. However, hard coking coal with high fluidity showed that the decomposition trend affects the difference in fluidity.

REFERENCES

1) A. K. Viswas: Principles of Blast Furnace Ironmaking, SBA Pub., Calcutta, India, (1981), 250.
2) M. F. Lin and M. T. Hong: *Fuel*, **65** (1986), 307.
3) W. H. Van niekerk and R. J. Dippenaar: *J. South African Inst. Min. Metall.*, **91** (1991), 53.
4) S. Nomura, T. Arima and K. Kato: *Fuel*, **83** (2004), 1771.
5) P. P. Kumar, S. C. Barman, S. Singh and M. Ranjan: *Ironmaking Steelmaking*, **35** (2008), 416.
6) A. A. Adeleke, R. S. Makan, S. Remyshak and K. M. Oluwasegun: *Pacific J. Sci. Technol.*, **13** (2012), 97.
7) M. A. Diez, R. Alvarez and C. Barrocanal: *Int. J. Coal Geology*, **50** (2002), 389.
8) R. Loison, P. Foch and A. Boyer: Coke Quality and Production, 2nd ed., Butterworths, London, UK, (1989), 62, 75.
9) I. C. Lewis: *Carbon*, **20** (1982), 519.
10) M. W. Haenel: *Fuel*, **71** (1992), 1211.
11) E. M. Hambly: The chemical structure of coal tar and char during devolatilization, Department of Chemical Engineering Brigham Young University, (1998), 4.
12) J. V. Ibarra, R. Moliner and A. J. Bonet: *Fuel*, **73** (1994), 918.
13) J. V. Ibarra, E. Munoz and R. Moliner: *Org. Geochem.*, **24** (1996), 725.
14) S. Nomura and K. M. Thomas: *Fuel*, **77** (1998), 829.
15) P. R. Solomon and R. M. Carangelo: *Fuel*, **60** (1981), 663.
16) P. B. Tooke and A. Grint: *Fuel*, **62** (1983), 1003.
17) P. C. Painter, M. Sobkowiak and J. Youtcheff: *Fuel*, **66** (1987), 973.
18) P. R. Solomon and R. M. Carangelo: *Fuel*, **67** (1988), 949.
19) M. A. Ahmed, M. J. Blesa, R. Juan and R. E. Vandenberghe: *Fuel*, **82** (2003), 1825.
20) W. Geng, T. Nakajima, H. Takanashi and A. Ohki: *Fuel*, **88** (2009), 139.
21) A. H. Clemens, T. W. Matheson, L. J. Lynch and R. Sakurovs: *Fuel*, **68** (1989), 1162.
22) M. D. Casal, A. I. Gonzalez, C. S. Canga, C. Barriocanal, J. J. Pis, R. Alvarez and M. A. Diez: *Fuel Process. Technol.*, **84** (2003), 47.
23) S. Yao, K. Zhang, K. Jiao and W. Hu: *Energy Explor. Exploit.*, **29** (2011), 1.
24) Y. Fujioka, M. Nishifuji, K. Saito and K. Kato: *Testu-to-Hagané*, **88** (2002), 29.
25) X. Qi, D. Wang, H. Xin and G. Qi: *Energ. Fuel.*, **27** (2013), 3130.
26) I. Noda: *Appl. Spectrosc.*, **44** (1990), 550.
27) I. Noda, A. E. Dowrey, C. Marcott and G. M. Story: *Appl. Spectrosc.*, **54** (2000), 237.
28) P. C. Painter, R. W. Snyder, M. Starsinic, M. M. Coleman, D. W. Kuehn and A. Davis: *Appl. Spectrosc.*, **35** (1981), 475.
29) L. Shi, Q. Liu, X. Guo, W. Wu and Z. Liu: *Fuel Process. Technol.*, **108** (2013), 125.
30) K. Kidena, M. Hiro, S. Murata and M. Nomura: *Energ. Fuel.*, **19** (2005), 224.